NACA

RESEARCH MEMORANDUM

FLIGHT TESTS TO DETERMINE THE DRAG OF FIN-STABILIZED PARABOLIC BODIES AT TRANSONIC AND SUPERSONIC SPEEDS

By

Sidney R. Alexander, Leo T. Chauvin,
and Charles B. Rumsey

Langley Memorial Aeronautical Laboratory
Langley Field, Va.

NATIONAL ADVISORY COMMITTEE FOR AERONAUTICS

WASHINGTON

April 21, 1948

NATIONAL ADVISORY COMMITTEE FOR AERONAUTICS

RESEARCH MEMORANDUM

FLIGHT TESTS TO DETERMINE THE DRAG OF FIN-STABILIZED PARABOLIC BODIES AT TRANSONIC AND SUPERSONIC SPEEDS

By Sidney R. Alexander, Leo T. Chauvin,
and Charles B. Rumsey

SUMMARY

Parabolic bodies of revolution of two fineness ratios were flight-tested in the transonic and supersonic range by the use of rocket propulsion. The basic parabolic shapes were of fineness ratios 10 and 15. Omitting the rear portion of the parabola of revolution to provide for the rocket jet resulted in actual body fineness ratios of 7.87 and 12. The models were stabilized by tail fins mounted at the base of the bodies.

The model of fineness ratio 7.87 was tested over a Mach number range of 0.58 to 1.19, and that of fineness ratio 12 over a range of 1.16 to 2.58. Curves of measured total drag coefficient plotted against Mach number are presented. Total drag coefficients for several Mach numbers, as computed prior to the tests, are included in order to indicate the reasonable accuracy that can be expected from such predictions.

The tests also proved the effectiveness of a simple "drag-separation" type booster arrangement.

INTRODUCTION

As part of the NACA program to investigate body shapes suitable for supersonic flight, the Langley Pilotless Aircraft Research Division has undertaken a program using the rocket-powered flight-test technique to determine the aerodynamic characteristics of two fin-stabilized, parabolic bodies of revolution. The body fineness ratios were chosen so as to make the experimental data comparable with results presented in a theoretical investigation of the drag of parabolic bodies at supersonic speeds (reference 1). The basic parabolic shapes were of fineness ratios 10 and 15. Omitting the rear portion of the parabola of revolution to provide for the rocket jet resulted in actual body fineness ratios of 7.87 and 12.

The purpose of the tests described herein was to determine the drag characteristics of the two models and incidentally prove the effectiveness of a simple "drag-separation" type booster arrangement. This paper presents the drag characteristics of blunt-ended, fin-stabilized, parabolic bodies of fineness ratios 7.87 and 12 for a Mach number range of 0.58 to 1.19 and 1.16 to 2.58, respectively. The values of total drag coefficient are compared at several Mach numbers with those determined from an independent estimation based on a prudent selection of pertinent theoretical and experimental literature.

The flight tests were conducted by Langley Pilotless Aircraft Research Division at its testing station at Wallops Island, Va.

MODELS

Two models of each configuration were constructed. These models will be designated "A" and "B." The bodies were of parabolic-arc profile with one end cut off to allow rocket-motor exhaust. Each body was stabilized by three untapered, 60° sweptback fins employing circular-arc sections equally spaced around the stern. The two models of the fineness-ratio 7.87 configuration were similar and were about 60 inches long and of all wooden construction. The fin thickness ratio t/c, measured normal to the leading edge, was 10 percent. The models of the fineness-ratio 12 configuration were about 65 inches long and of wood and metal construction. The A model fin thickness ratio, for structural reasons, was 20 percent normal to the leading edge. For the B model, however, the fins were reduced to a thickness ratio of 10 percent. Figure 1 shows the general arrangement of the model configurations.

All models were propelled by 3.25-inch MK-7 aircraft rocket motors.

TESTS

The testing technique was identical to that described in reference 2. The two similar models of the smaller fineness-ratio bodies were launched from a zero-length-type launcher set at an elevation angle of 80°. (See figs. 2 and 3.) The purpose of firing two models was to insure the consistency of the velocity data secured by tracking the models with a Doppler velocimeter radar unit located near the launching site.

The fineness-ratio 12 model A was launched in the same manner as the two models of the smaller fineness ratio bodies. (See fig. 3(b).) In order to attain higher Mach numbers than those attained for the A model, the B model was launched under the power of a 5-inch, light-weight, high-velocity aircraft-rocket-motor booster. This booster was attached to the model by a simple finger-type arrangement (fig. 4) and, at the cessation of thrust, separated under application of its own drag and/or the sustaining rocket motor's thrust. A view of this model on its launcher is shown as figure 5. Both models were tracked in flight with the Doppler velocimeter.

The density and speed of sound for the determination of the drag coefficient and Mach number were obtained from radiosonde observations made at the time of firing.

The variation of the test Reynolds number (based on body length) with Mach number is presented in figure 6 for both model configurations.

All launchings and flights were satisfactory. The performance of the drag-separation type booster indicated the practicability of this type for use with small high-speed test vehicles.

RESULTS AND DISCUSSION

Experimental Results

The velocity-time curves, as obtained from the data secured by the radar unit, are presented in figure 7 for the two fineness-ratio configurations. The small difference between the curves for the fineness-ratio 7.87 configuration can be attributed to slight differences in weight and motor performance. By graphically differentiating the velocity-time curves from beyond the maximum velocity point and taking into account the atmospheric conditions and the weight of the model after the propellant had been expended, values of drag coefficient, based on maximum frontal area exclusive of the fins, were calculated. These results are presented in figure 8 for the two body fineness ratios investigated. Considering the curves for the A and B models of the 7.87-fineness-ratio configuration (fig. 8(a)) which should be comparable, it can be seen that, although the curves diverge at the higher Mach numbers tested, the agreement between the curves is good and in keeping with the accuracy of this general technique as ascertained in reference 2.

Examination of figure 8(b) reveals an increment in drag coefficient between the A and B models of the fineness-ratio 12 configuration that can be mainly attributed to difference in fin-profile thickness between the models and is of the order predicted by the two-dimensional theory. The slight rise in the curve of the B model near a Mach number of 1.5 can be attributed to the fins. For the case of an isolated fin, the rise should occur at a Mach number of 2.0 for 60° of sweepback (when the Mach line lies on the leading edge), but in this case, because of the increased velocity over the fins due to their location on the body, this condition occurs at a lower free-stream Mach number as is indicated.

Drag Estimates

Previous to the firings, an estimate of the total drag of each tested configuration was made using generally available pertinent literature. The purpose was to obtain some indication of the degree of accuracy to be expected from what might be considered a first-order approach towards estimating the total drag of flight configurations at supersonic speeds. No attempt was made to estimate the drag coefficients by the outlined method at a Mach number lower than 1.2 since in this range the validity of the linearized theory becomes questionable.

The estimate was obtained in the following manner:

Body pressure drag.- The pressure drag over the surface of the bodies was calculated from the surface pressure distribution which was arrived at by the method outlined in reference 1.

Body viscous drag.- The viscous drag coefficient was obtained from reference 3 using the assumption of a laminar boundary layer over the forward 30 percent of the body and a turbulent boundary layer over the remaining part. A check of the order of magnitude of the result was obtained from reference 4. Assuming a turbulent boundary layer over the entire body would result in an increase of 25 percent in viscous drag coefficient.

Base pressure drag.- In estimating the base pressure for fineness-ratio 7.87 models, comparable bodies of references 5 and 6 were considered in order to ascertain the effect on base pressure of the relatively low Reynolds numbers of reference 5. Since the effect appeared to be negligible, base pressure obtained from tests of a body comparable to that being considered was used directly from reference 5.

In estimating the base drag for fineness-ratio 12 models at the higher Mach numbers reached by this configuration, approximations of base pressure were obtained from the Boeing Aircraft Company.

The values of base pressure coefficients were converted to drag coefficients based on the respective body frontal areas, exclusive of the fins.

Fin drag.- The fin drag for fineness-ratio 7.87 models was based on the experimental data of reference 7. No attempt was made to estimate the body-fin interference effects due to the uncertainty of these conditions, and it was further felt that the difference to the fin drag and particularly the total drag, realized by attempting to take into account these interference effects, would not be in keeping with the objective of these estimates.

The fin drags for fineness-ratio 12 models were calculated using the methods presented in references 8 and 9 after determining the velocity field around the fins from reference 1.

The comparison obtained between the results of the experimental flight tests and the independent drag estimates is presented in figure 9. Examination of the figure reveals a discrepancy between the estimated and experimental total drag coefficient values of about 14 percent for the fineness-ratio 7.87 configuration. For the fineness-ratio 12 configuration the discrepancy between the estimated and experimental values is about 12, 9.5, 10, and 1.5 percent at Mach numbers of 1.2, 1.5, 2.0, and 2.5, respectively. These results, in general, indicate that the components of drag for a fin-stabilized body in the supersonic range can be calculated with sufficient accuracy for first-order approximations by the use of existing data.

CONCLUDING REMARKS

Experimental values of the total drag coefficients were obtained for fin-stabilized, blunt-ended, parabolic bodies of revolution of fineness ratios 7.87 and 12. Values for the fineness-ratio 7.87 configuration were obtained through a Mach number range of 0.58 to 1.19, and for the fineness-ratio 12 configuration through a Mach number range of 1.16 to 2.58.

Comparison of the experimental values of drag coefficient and the estimated values calculated prior to the tests show that the components of drag for a fin-stabilized body in the supersonic range can be calculated with sufficient accuracy for preliminary design by the use of existing theoretical and experimental data.

Langley Memorial Aeronautical Laboratory
National Advisory Committee for Aeronautics
Langley Field, Va.

REFERENCES

1. Jones, Robert T., and Margolis, Kenneth: Flow over a Slender Body of Revolution at Supersonic Velocities. NACA TN No. 1081, 1946.

2. Alexander, Sidney R., and Katz, Ellis: Flight Tests to Determine the Effect of Length of a Conical Windshield on the Drag of a Bluff Body at Supersonic Speeds. NACA RM No. L6J16a, 1947.

3. Falkner, V. M.: A New Law for Calculating Drag. The Resistance of a Smooth Flat Plate with Turbulent Boundary Layer. Aircraft Engineering, vol. XV, no. 169, March 1943, pp. 65–69.

4. von Kármán, Theodor, and Moore, Norton B.: Resistance of Slender Bodies Moving with Supersonic Velocities, with Special Reference to Projectiles. Trans. A.S.M.E., vol. 54, no. 23, Dec. 15, 1932, pp. 303–310.

5. Chapman, Dean R., and Perkins, Edward W.: Experimental Investigation of the Effects of Viscosity on the Drag of Bodies of Revolution at a Mach Number of 1.5. NACA RM No. A7A31a, 1947.

6. Thompson, Jim Rogers, and Marschner, Bernard W.: Comparative Drag Measurements at Transonic Speeds of an NACA 65–006 Airfoil and a Symmetrical Circular–Arc Airfoil. NACA RM No. L6J30, 1947.

7. Ellis, Macon C., Jr., and Hasel, Lowell E.: Preliminary Tests at Supersonic Speeds of Triangular and Sweptback Wings. NACA RM No. L6L17, 1947.

8. Harmon, Sidney M., and Swanson, Margaret D.: Calculations of the Supersonic Wave Drag of Nonlifting Wings with Arbitrary Sweepback and Aspect Ratio. Wings Swept Behind the Mach Lines. NACA TN No. 1319, 1947.

9. Harmon, Sidney M.: Theoretical Supersonic Wave Drag of Untapered Sweptback and Rectangular Wings at Zero Lift. NACA TN No. 1449, 1947.

[redacted]

Model	Center-of-gravity station at launching, in.
"A"	42.38
"B"	42.00

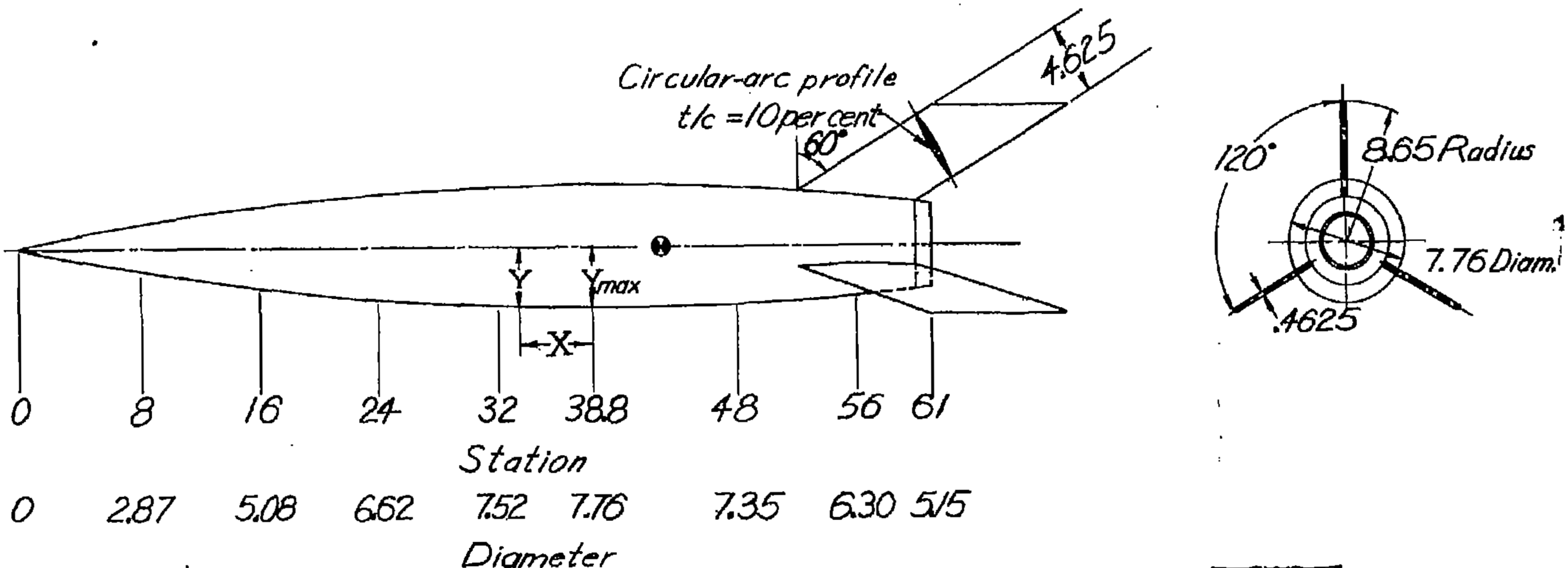

Fuselage profile equation

$$Y = Y_{max} - 0.002577X^2$$

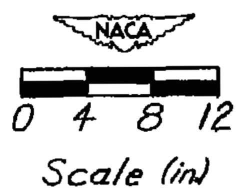

(a) Fineness-ratio 7.87 configuration.

[redacted]

Figure 1.- General configuration of test models.

[redacted]

Model	Center-of-gravity station at launching, in
"A"	44.75
"B"	43.25

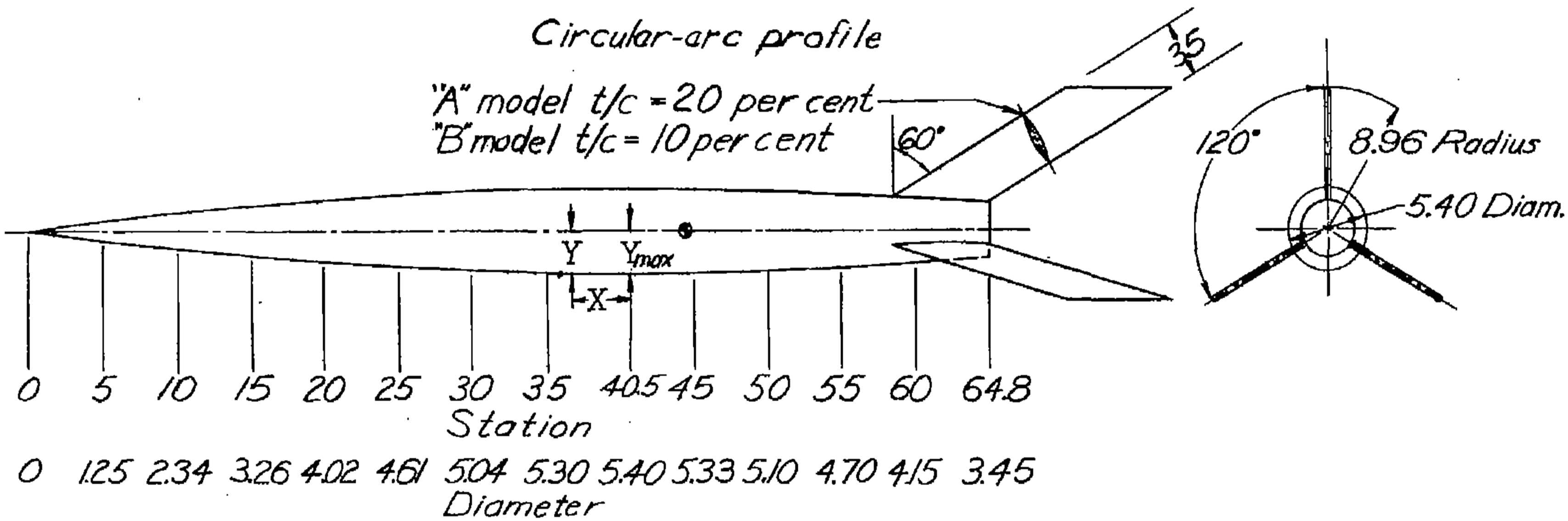

Fuselage profile equation

$$Y = Y_{max} - 0.001646 X^2$$

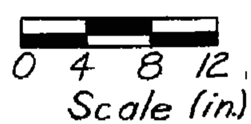

(b) Fineness-ratio 12 configuration.

[redacted]

Figure 1. - Concluded.

Figure 2.- View of launcher for the fineness-ratio 7.87 models and for the fineness-ratio 12 "A" model.

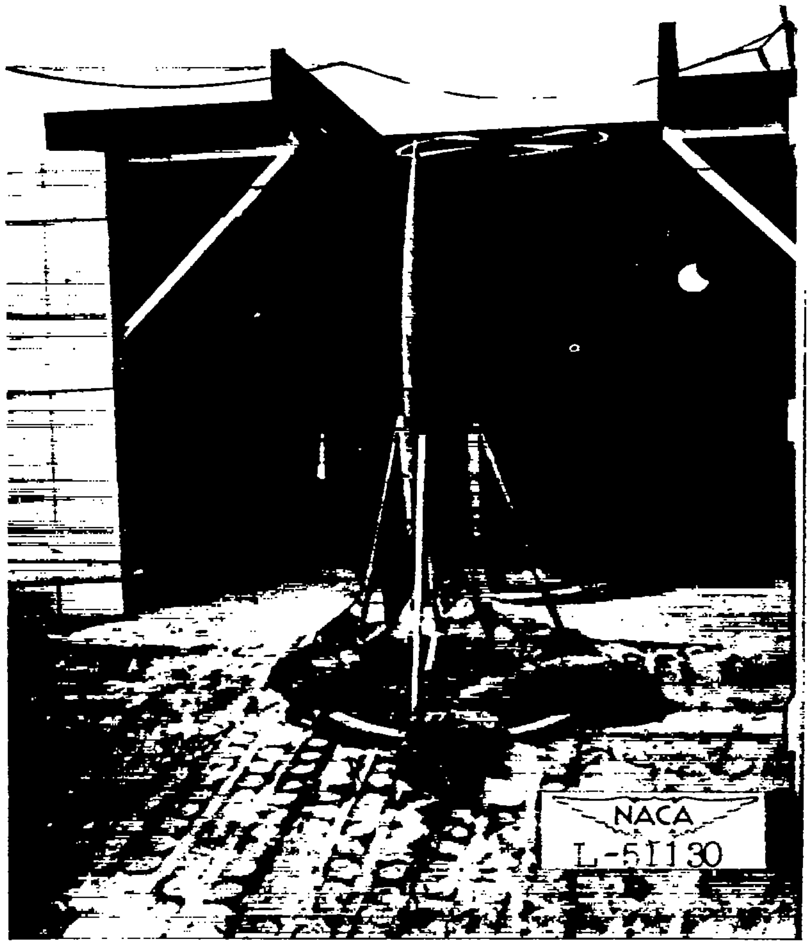

(a) Fineness-ratio 7.87 model.

Figure 3.- Views of models in launcher.

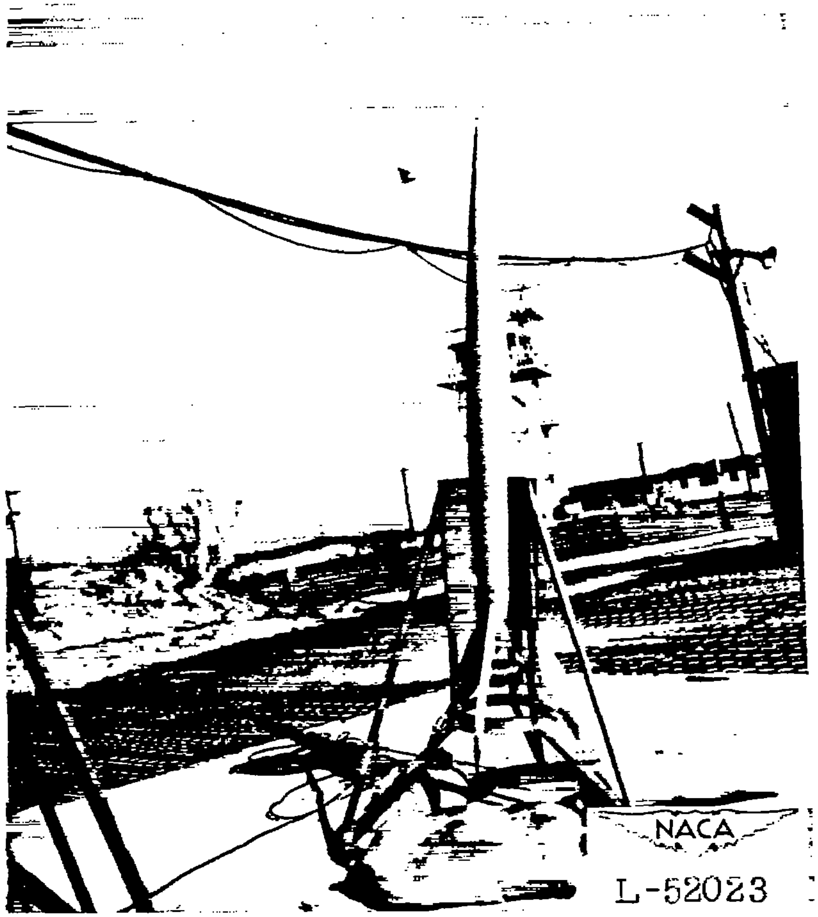

(b) Fineness-ratio 12 "A" model.

Figure 3.- Concluded.

[redacted]

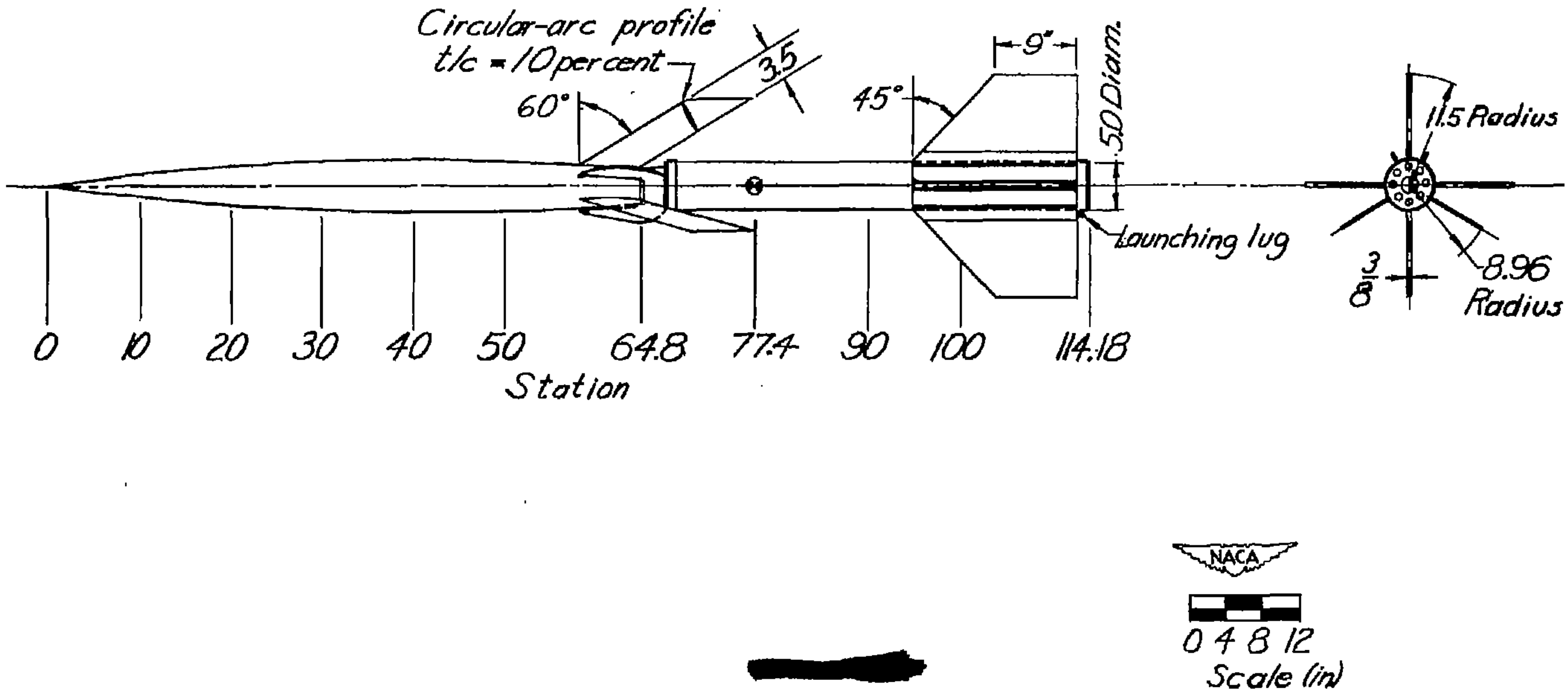

[redacted]

Figure 4.-General configuration of fineness-ratio 12 "B" model with booster rocket.

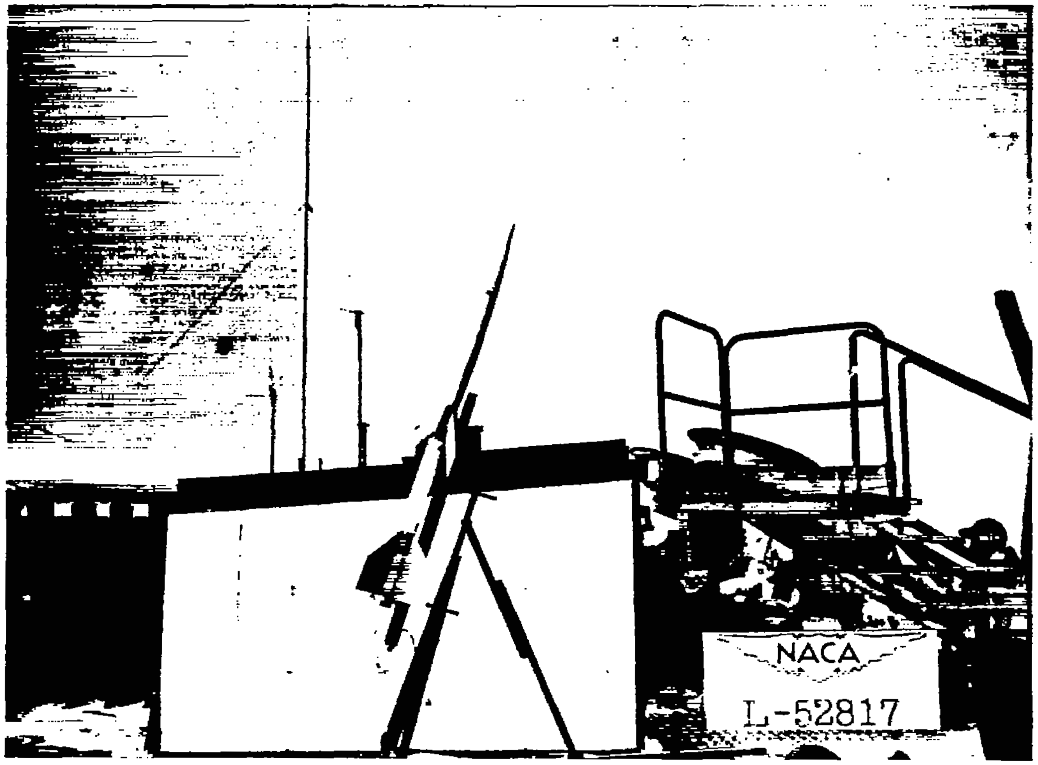

Figure 5.- View of fineness-ratio 12 "B" model in launcher.

[redacted]

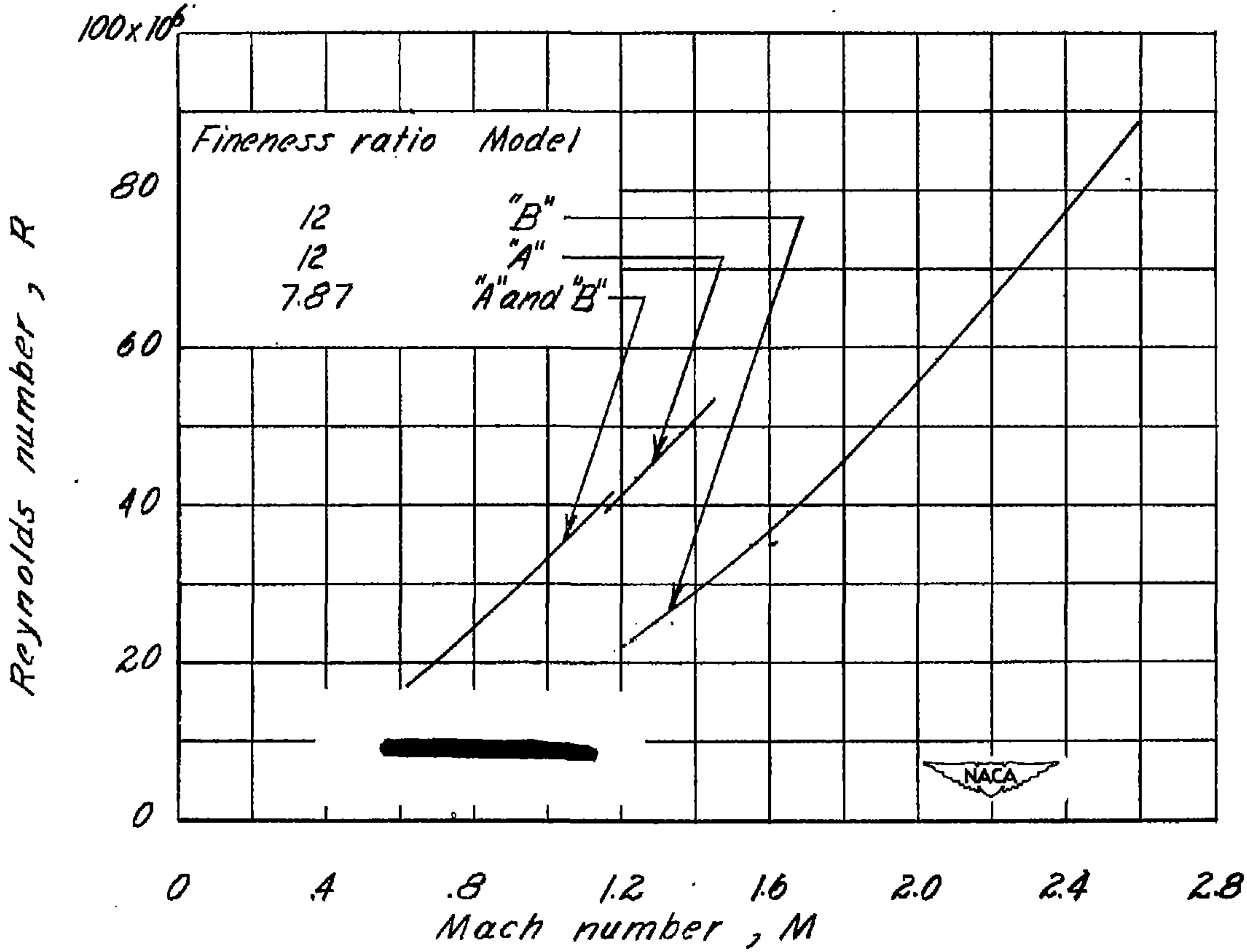

Figure 6.- Variation of Reynolds number with Mach number for both fineness-ratio configurations.

[redacted]

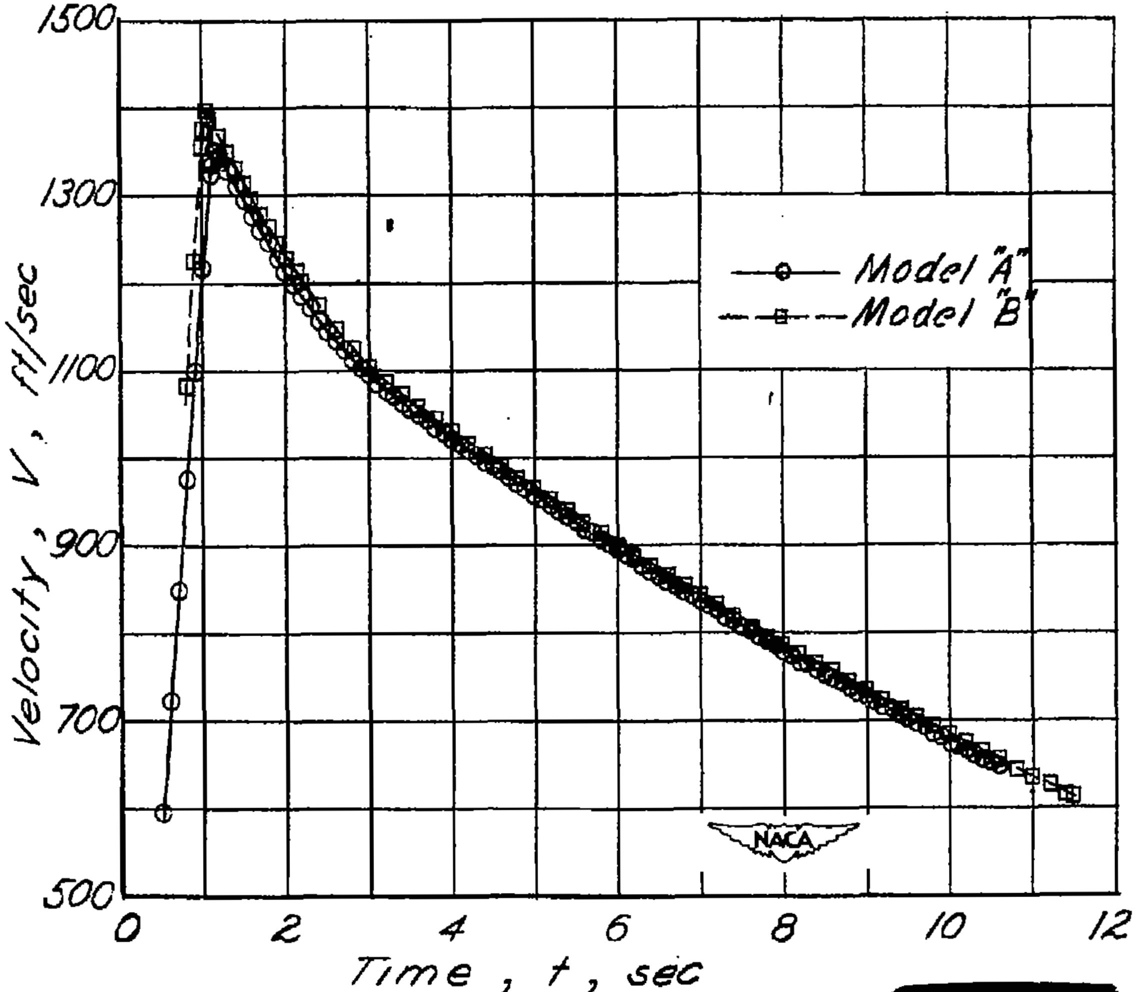

[redacted]

(a) Fineness-ratio 7.87 configuration.

Figure 7.- Velocity-time relations for the two body fineness-ratio configurations investigated.

[redacted]

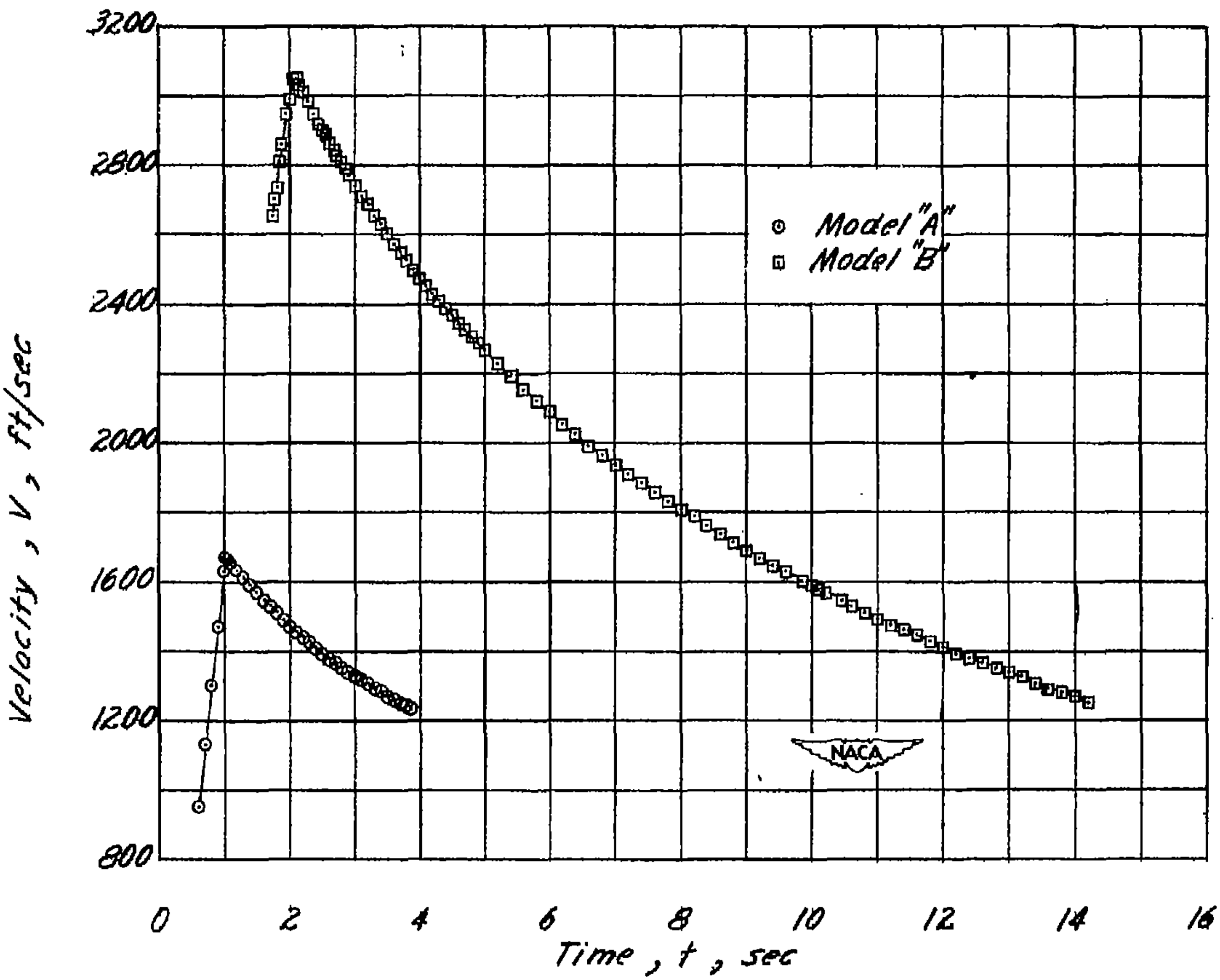

[redacted]

(b) Fineness-ratio 12 configuration.
Figure 7.-Concluded.

[redacted]

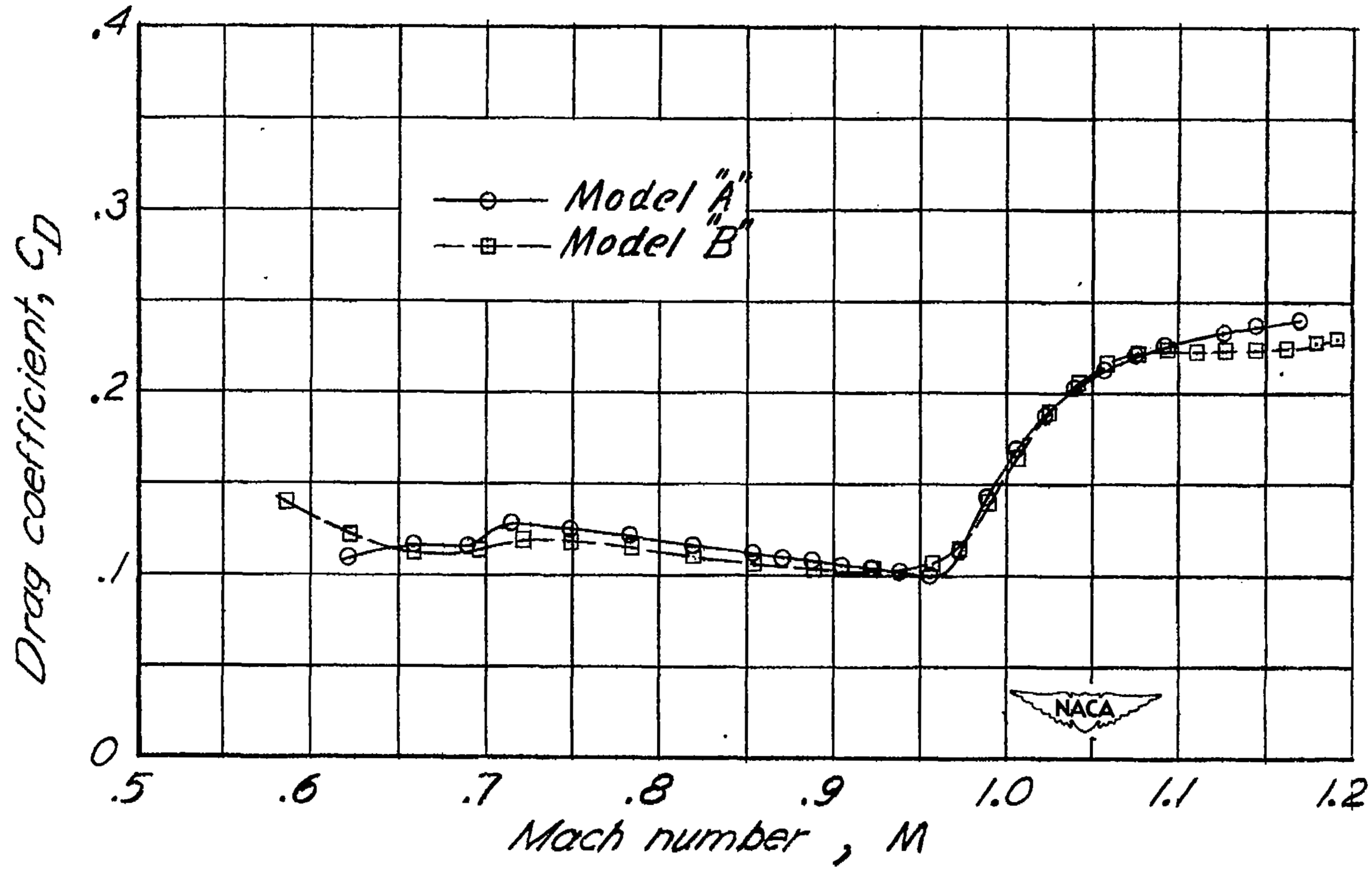

(a) Fineness-ratio 7.87 configuration. [redacted]

Figure 8.- Drag coefficients for the two fineness-ratio bodies investigated.

[redacted]

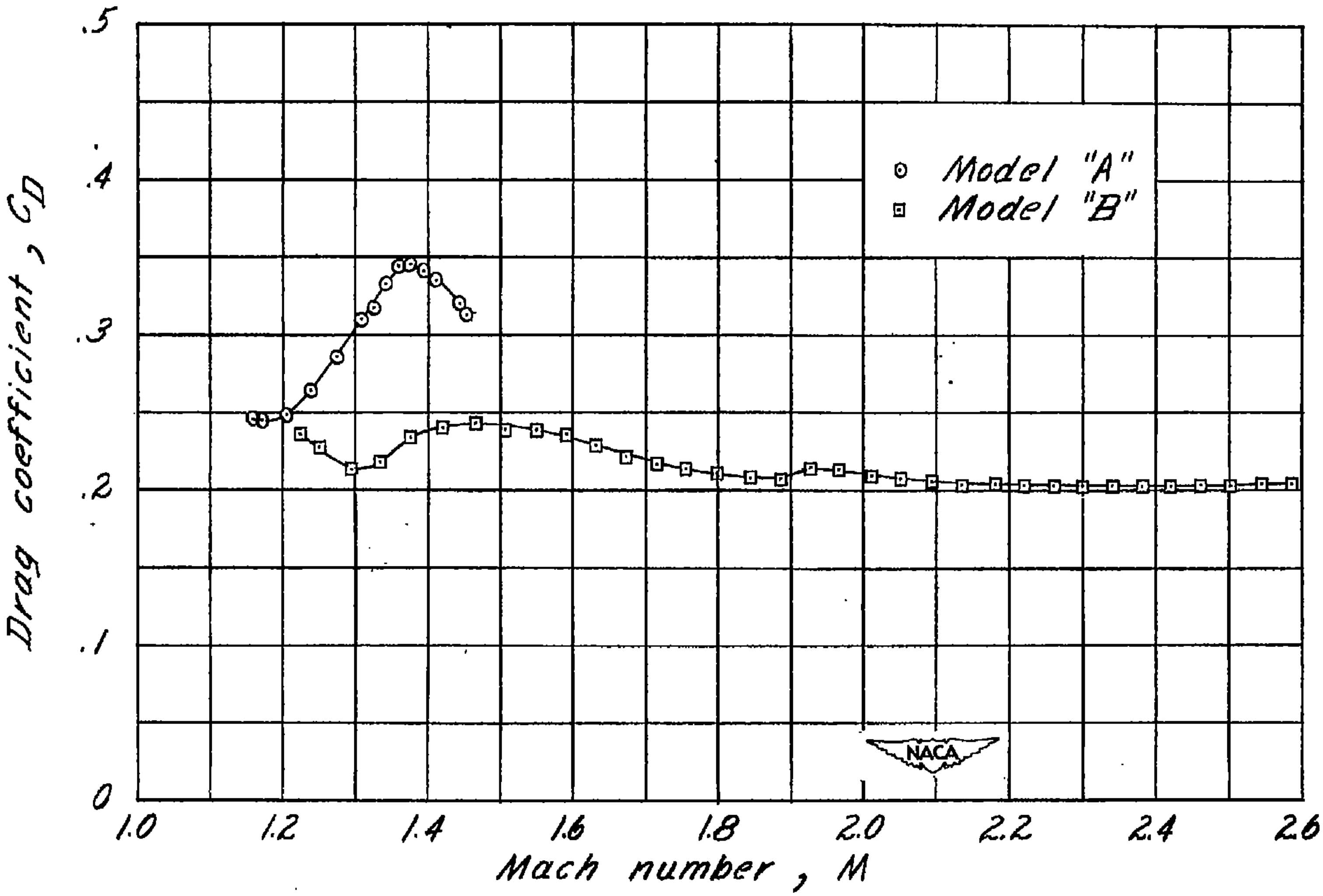

[redacted]

(b) Fineness-ratio 12 configuration.

Figure 8.- Concluded.

[redacted]

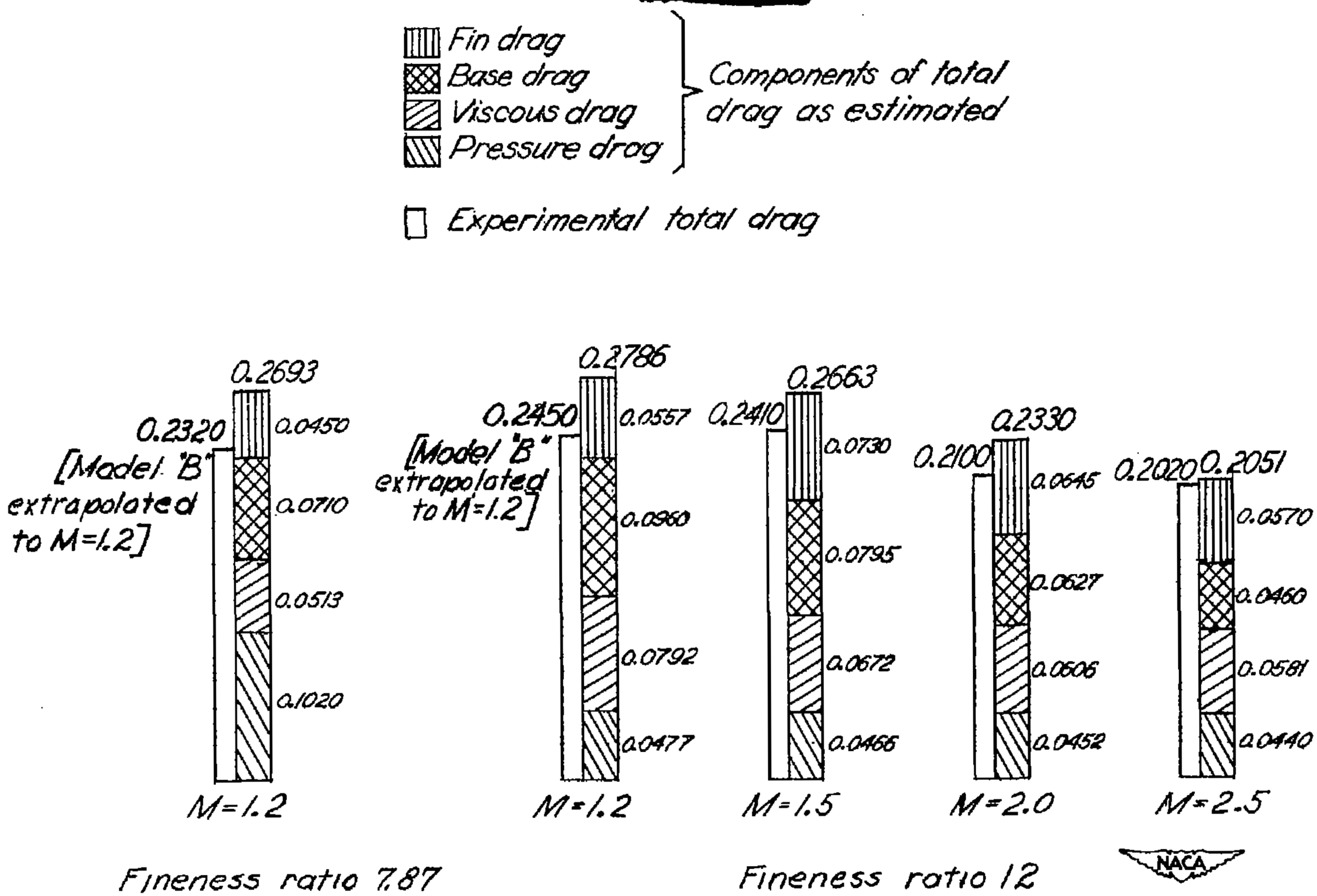

[redacted]

Figure 9.- Comparison of experimental and estimated values of drag coefficient.